

# Electrical Properties of Gamma-Irradiated, Pure, and Nickel Chloride-Doped Polyvinyl Alcohol Films

A. SHEHAP,<sup>1</sup> R. A. ABD ALLAH,<sup>2</sup> A. F. BASHA,<sup>1</sup> F. H. ABD EL-KADER<sup>1</sup>

<sup>1</sup> Department of Physics, Faculty of Science, Cairo University, Giza, Egypt

<sup>2</sup> Department of Physics, Faculty of Industrial Education, High Education Ministry, Cairo, Koba, Egypt

Received 3 March 1997; accepted 12 September 1997

**ABSTRACT:** The electrical transport properties, such as direct current (dc) electrical conductivity ( $\sigma$ ), dielectric constant ( $\epsilon'$ ), and dc current–time characteristics of unirradiated and  $\gamma$ -irradiated pure and NiCl<sub>2</sub>-doped PVA were studied in the temperature range of 26–155°C. Quantitative analysis was carried out to determine the thermal activation energy of the conduction process, drift mobility, and carrier concentration. The thermally activated mobility of charge carriers is confirmed from calculations of drift mobility at different  $\gamma$ -doses and temperatures. The results obtained revealed that  $\gamma$ -irradiation enhances the conductivity. The dielectric constant data at different temperatures before and after irradiation can be attributed mainly to the changes in the intra- and intermolecular interactions. The dc conductivity at 30 and 40°C, activation energy in low temperature region I, and  $\epsilon'_{\max}$  for 20 wt % NiCl<sub>2</sub> proved to be dose-dependent. The obtained data suggests that these materials may have an application in dosimetry. © 1998 John Wiley & Sons, Inc. *J Appl Polym Sci* 68: 687–698, 1998

**Key words:** electrical properties of PVA films

## INTRODUCTION

One of the goals of material research is to create new materials with physical properties tailored to a particular application and to understand the physical mechanisms that determine these properties. A metal introduced into a polymer chain, as a rule, causes improvement of the polymer behavior and often even brings about new performance properties. Transition elements may be present in polymers in various quantities and forms and may be introduced deliberately or as impurities.

Polyvinyl alcohol (PVA) is an important material in view of its large-scale applications, such

as surgical devices, sutures, hybrid islet transplantation,<sup>1,2</sup> implantation, and as synthetic articular cartilage in reconstructive joint surgery.<sup>3</sup>

Electrical properties constitute one of the most convenient and sensitive methods for studying the polymer structure.<sup>4–7</sup> They are influenced not only by the structure and nature of a dopant but also by the doping concentration and procedure.<sup>8–12</sup> In addition,  $\gamma$ -irradiation has become one of the most common processes producing modifications in their physical, chemical, and morphological structures.<sup>13–16</sup>

Accordingly, factors that have an appreciable effect on the polymer structure must be carefully studied. Hence, in the present work, it was proposed to study the effect of both dopant concentration and  $\gamma$ -irradiation on the electrical properties of PVA films. This work is a continuation to a series of studies carried out by our team of work.<sup>5,6,12</sup>

Correspondence to: F. H. Abd El-Kader.

*Journal of Applied Polymer Science*, Vol. 68, 687–698 (1998)  
© 1998 John Wiley & Sons, Inc.

CCC 0021-8995/98/050687-12

## EXPERIMENTAL

The PVA and  $\text{NiCl}_2 \cdot 6 \text{H}_2\text{O}$  used in this work were obtained from BDH chemicals and Hayashi Chemical Industries, Japan, respectively. The components (nominally free from impurities) were dissolved in distilled water and PVA– $\text{NiCl}_2$  samples were made in weight percentages (wt %) of 5, 10, and 20% of  $\text{NiCl}_2 \cdot 6 \text{H}_2\text{O}$ . Distilled water solution was cast on glass plate and dried in an air oven at  $40^\circ\text{C}$  for 48 h in order to minimize gelation effects. Samples of  $0.25 \pm 0.005$  mm were irradiated by different doses of  $\gamma$ -rays in the range of  $1\text{--}20 \times 10^4$  Gy using  $^{60}\text{Co}$  source at room temperature and a constant dose rate. The dc conductivity,  $\sigma$ , was measured by applying a constant voltage of 1 V and measuring the conduction current using a Keithley electrometer, model 616. For ohmic contacts, silver paste ( $R < 4 \Omega$ ) was spread on the sample surface as electrodes and used as an adhesive to attach the leads (silver wire).

The dielectric constant,  $\epsilon'$ , was measured using 1 kHz capacitance bridge (Type WEKYNE KERR B 900) with a least count 1 pF. The dielectric constant was calculated from the capacitance  $c$  using the following formula:

$$\epsilon' = \frac{cd}{\epsilon_0 A} \quad (1)$$

where  $d$  is the thickness of the film,  $A$  is the cross-sectional area of the film surface, and  $\epsilon_0$  is the free-space permittivity. Measurements of  $\sigma$  and  $\epsilon'$  were made at a moderate heating rate  $1 \text{ K min}^{-1}$  from 293 up to 433 K.

## RESULTS AND DISCUSSION

### DC Electrical Conductivity

The radiation-induced dc electrical change could, in principle, be used as a measure of  $\gamma$ -rays absorbed doses. This induced dc electrical conductivity ( $\sigma$ ) is carefully studied in the dose range up to  $2 \times 10^5$  Gy. The variation of  $\log \sigma$  on  $1/T$  for the unirradiated and irradiated pure and doped PVA films with different concentrations of  $\text{NiCl}_2$  (5, 10, and 20 wt %) were studied. Figure 1 shows the dc conductivity spectra for the pure PVA samples before and after  $\gamma$ -irradiation in the range  $1$

$\times 10^4\text{--}2 \times 10^5$  Gy. Evidently, all the plots of Figure 1 indicate the maintenance of three segments obeying the normal Arrhenius equation. It can be seen that the general trend of the conductivity–temperature curves is similar; the curves themselves sometimes overlap and intersect at a relatively higher temperature range. From the inspection of this figure, it is clear that the dc conductivity increases as the temperature and  $\gamma$ -dose increases. However, the sample irradiated at  $2 \times 10^5$  Gy shows a decrease in  $\sigma$  when compared with samples irradiated with  $1 \times 10^5$  and  $1 \times 10^4$  Gy at higher temperatures.

The induced changes in  $\sigma$  at 30 and  $40^\circ\text{C}$  are shown to be dose-dependent and can be attributed to the creation of induced charge carriers in the PVA matrix (see the inset of Figure 1). Results shown in the inset of Figure 1 indicate that the induced rate of change in  $\sigma$  is enhanced for sample irradiated at doses less than  $10^4$  Gy, while, as the dose becomes higher, the rate of induced change in dc conductivity becomes smaller. This dependence of the dc conductivity on the  $\gamma$ -dose might be explained as follows. At the beginning, increasing the  $\gamma$ -dose would result in an increase in the number of charge carriers created. This increasing number of carriers will continue to take place as  $\gamma$ -dose increases until we approach a situation at which most of the possible charge carriers are already created. After this threshold dose limit, we might expect no more increase in the dc conductivity, and a saturation limit might be achieved. Unfortunately, reaching this saturation limit is difficult to follow at a high temperature region because of the existence of more complicated conduction mechanisms. The increase in conductivity at high temperature may be accounted for by the liberation of electrons or ions through the amorphous region of PVA, and/or, probably, the internal stresses in the doped sample may also play a role in the motion of charge carriers.<sup>17,18</sup> As a result of  $\gamma$ -irradiation, ions and free radicals are formed and partially trapped in the bulk of the material. Further, the irradiation was carried out in air, and, hence, the formed gaseous ions around the films may produce space charge in the surface of the specimen.<sup>19</sup> Moreover, there is a monotonic decrease in the position of the glass transition temperature for unirradiated sample ( $T_g \approx 340 \text{ K}$ ) with radiation so that the total shift is about 19 K. It is attributed to the generation of low-molecular-weight species and free chain ends with radiation.<sup>20</sup> It is known that

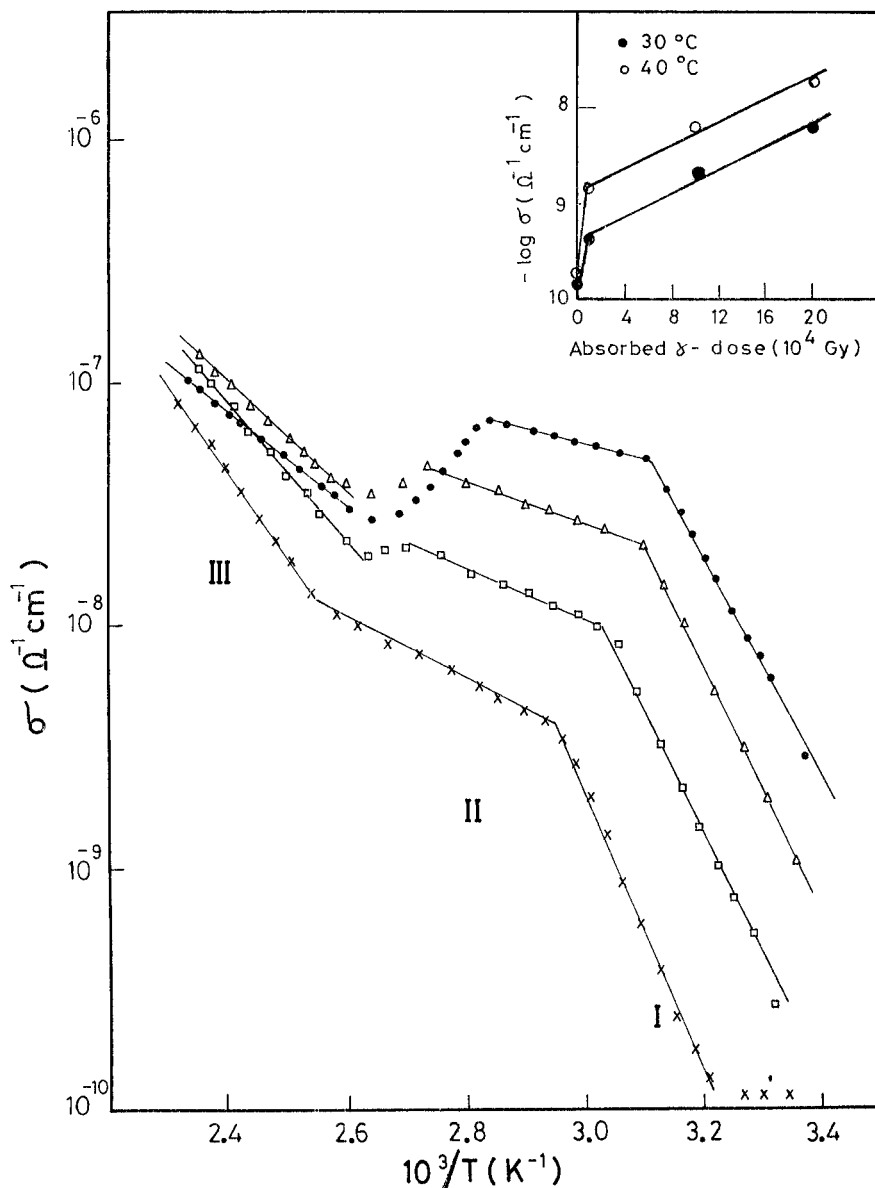


**Figure 1** Variation of the electrical conductivity of unirradiated and irradiated pure PVA samples with the reciprocal of temperature at 1 V: (×) unirradiated, (□)  $1 \times 10^4$  Gy, (△)  $1 \times 10^5$  Gy, and (●)  $2 \times 10^5$  Gy.

many halogen-containing polymers with the halogen bonded to the main chain and/or side chains readily undergo  $\gamma$ -radiolysis.<sup>21,22</sup>

For the 5 wt %  $\text{NiCl}_2$ -doped PVA samples, the plots of  $\log \sigma$  against  $1/T$  depict generally the same behavior as in the case of pure PVA samples (see Fig. 2). However, the electrical conductivity for pure PVA samples is less than that for the counterparts in 5 wt %  $\text{NiCl}_2$ -doped PVA in regions I and II. Nickel ions are coordinated through ionic bonds with the hydroxyl group be-

longing to the different chains in PVA.<sup>12</sup> This, in turn, reduces the intermolecular interaction between chains and expands the space between them. In other words, the addition of nickel increases the volume required for ionic carriers to drift in the polymer. This leads to an increase in the ionic mobility and a reduction in the activation energy. This is in complete accordance with the results observed. It has been thought that the nonuniform doping causes heterogeneity, which leads to the formation of nonstoichiometric

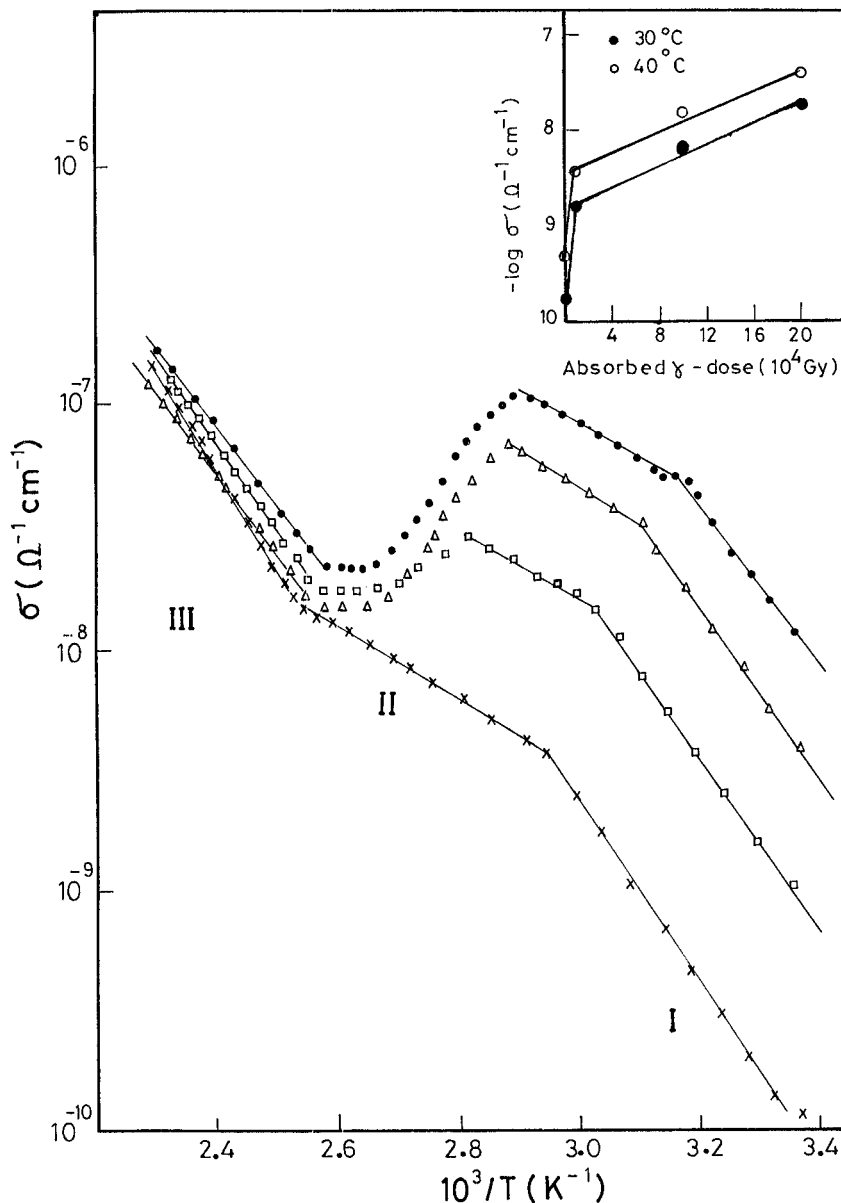


**Figure 2** Variation of electrical conductivity of unirradiated and irradiated PVA samples containing 5 wt %  $\text{NiCl}_2$  with the reciprocal of temperature at 1 V: ( $\times$ ) unirradiated, ( $\square$ )  $1 \times 10^4$  Gy, ( $\triangle$ )  $1 \times 10^5$  Gy, and ( $\bullet$ )  $2 \times 10^5$  Gy.

charge-transfer complexes between the polymer and dopant.<sup>5</sup>

In the case of the samples with both concentrations of 10 and 20 wt %  $\text{NiCl}_2$ , the temperature dependence of the electrical conductivity before and after irradiation generally describes a nearly similar behavior. Figure 3 illustrates, as a representation, the variation of  $\sigma$  versus  $1/T$  for PVA containing 20 wt %  $\text{NiCl}_2$ . One notes that the intermediate region II of the plots forms a wide min-

imum between two regular regions of behavior, namely, I and III. At low and high temperature regions, the induced rate of change in  $\sigma$  is greatest for sample irradiated at  $1 \times 10^5$  Gy while the rate of induced change in  $\sigma$  becomes smaller at higher dose  $2 \times 10^5$  Gy. Such a variable response to  $\gamma$ -irradiation could be accounted for by its relatively high Ni content. The properties of the amorphous phase obviously play a major role in determining the overall response of the material.<sup>4,23</sup> The inset

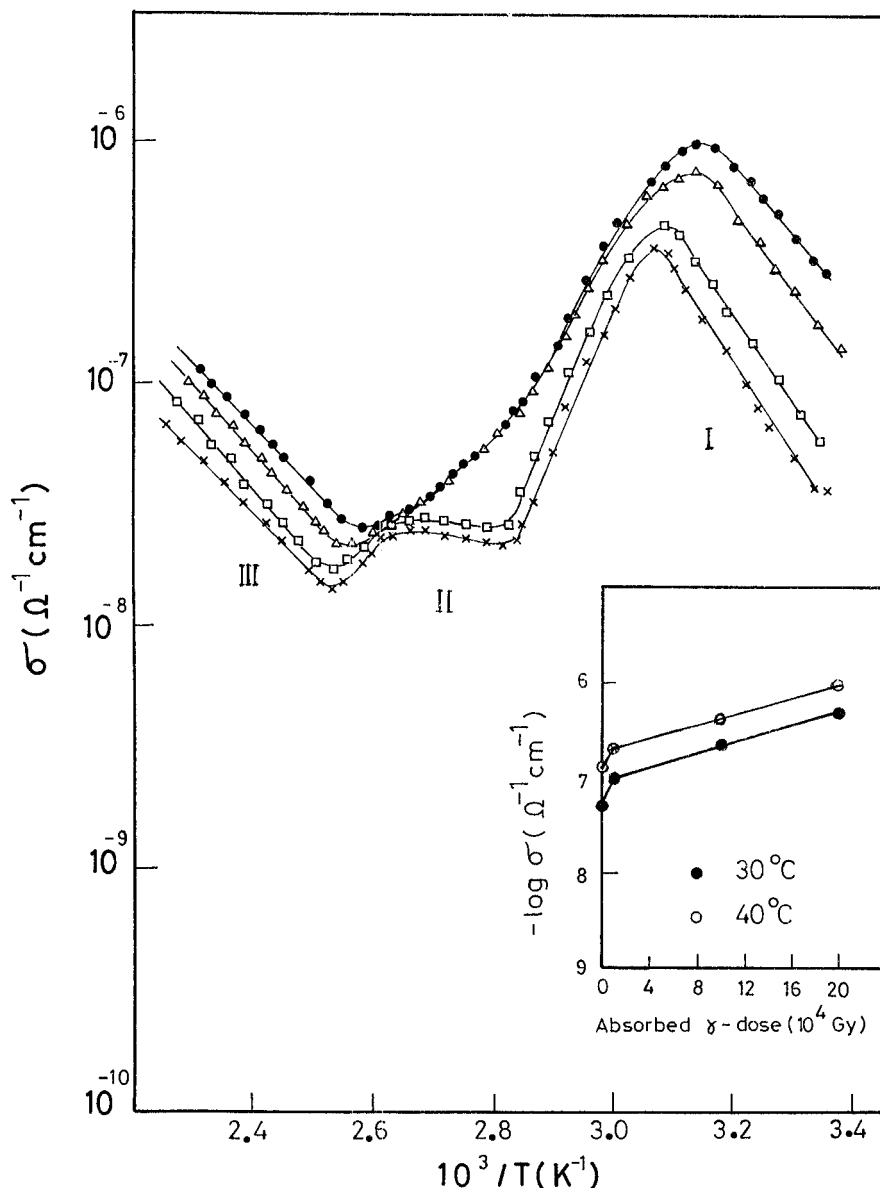


**Figure 3** Variation of the electrical conductivity of unirradiated and irradiated PVA samples containing 20 wt %  $\text{NiCl}_2$  with reciprocal of temperature at 1 V: ( $\times$ ) unirradiated, ( $\square$ )  $1 \times 10^4$  Gy, ( $\triangle$ )  $1 \times 10^5$  Gy, and ( $\bullet$ )  $2 \times 10^5$  Gy.

of Figure 3 shows that the induced change in  $\sigma$  is dose-dependent at temperatures 30 and 40°C.

Doped specimens showed larger conductivities in comparison with undoped specimens and with the increase in film temperature. This result is generally consistent with that previously reported in the literature.<sup>6</sup> Diffusion of the dopant into the polymer matrix plays an important role in the conduction process. If the dopants are not distributed homogeneously to electron donor sites, it will cause partial ionization, and heterogeneity would

create small conducting domains separated by some insulating regions of undoped polymer in such a segment rather than by hopping between localized states.<sup>11</sup>

The data of dc conductivity show that the carrier concentration increases with  $\gamma$ -irradiation (see Figs. 1–3). This is because the effect of ionizing  $\gamma$ -irradiation on polymer is to rupture chemical bonds and create energetic free electrons, ions, and radicals, which are able to migrate through the network, leading to a change in electrical conductivity.

**Table I** Values of the Activation Energy Calculated from DC Conductivity Measurements

Sample	Activation Energy (eV)											
	Unirradiated			$1 \times 10^4$ Gy			$1 \times 10^5$ Gy			$2 \times 10^5$ Gy		
	I	II	III	I	II	III	I	II	III	I	II	III
PVA	1.18	0.29	0.69	1.05	0.22	0.61	1.02	0.18	0.43	0.87	0.15	0.38
PVA + 5 wt % NiCl <sub>2</sub>	0.81	0.32	0.79	0.58	0.28	0.73	0.56	0.29	0.69	0.53	0.29	0.65
PVA + 10 wt % NiCl <sub>2</sub>	0.73	0.25	0.54	0.72	0.10	0.52	0.68	—	0.48	0.66	—	0.45
PVA + 20 wt % NiCl <sub>2</sub>	0.78	0.14	0.51	0.65	0.08	0.57	0.67	—	0.57	0.60	—	0.54

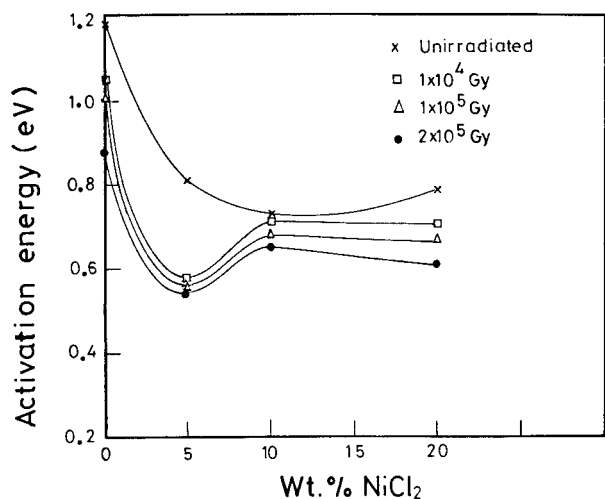
The conduction activation energy  $\Delta E$  can be estimated from the slope of  $\log \sigma$  versus  $1/T$  plot using the following equation:

$$\sigma = \sigma_0 \exp(-\Delta E/KT) \quad (2)$$

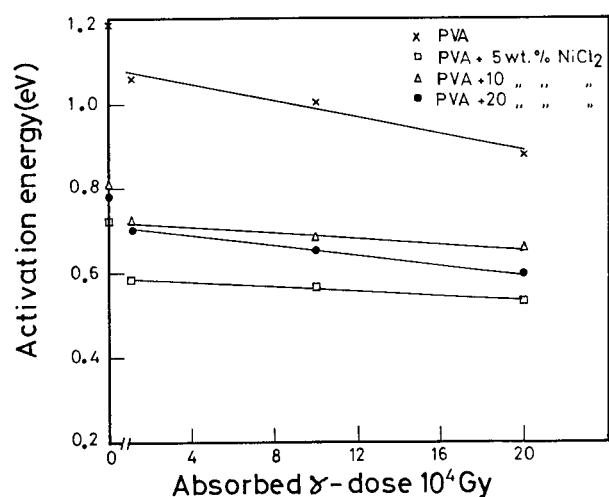
where  $\sigma_0$  is a constant,  $\Delta E$  is the thermal activation energy, and  $K$  is Boltzmann's constant. The activation energies evaluated for the unirradiated and irradiated samples are listed in Table I. It is obvious that the values of the activation energy vary as a function of the absorbed dose; they decrease with increasing  $\gamma$ -dose for each particular sample.

Figure 4 shows the variation in activation energy with the dopant concentration for unirradiated and irradiated samples. It is clear from the figure that the activation energy showed a mini-

mum at a concentration of 5 wt % NiCl<sub>2</sub> for irradiated samples and at a concentration of 10 wt % NiCl<sub>2</sub> for unirradiated samples. The decrease in the activation energy upon doping with nickel chloride may be attributed to the increase in the crystallinity of the polymer due to the alignment of the entangled chains in the amorphous region as a result of electrostatic interaction between the negatively charged hydroxyl groups and positive nickel ions. In addition,  $\gamma$ -irradiation seems capable to make some sort of variation in the amorphous regions reflecting a change in the structure of PVA-NiCl<sub>2</sub> system. On the other hand, the increase in activation energy at a higher concentration can be explained as being due to the formation of molecular aggregates of nickel chloride. The charge carriers become more localized, which gives the increase in the trapped carrier density.



**Figure 4** The variation of the activation energy of unirradiated and irradiated samples as a function of wt % NiCl<sub>2</sub> in the low temperature region 1.



**Figure 5** Variation of the activation energy of pure and doped PVA samples with the absorbed  $\gamma$ -dose in the low-temperature region 1.

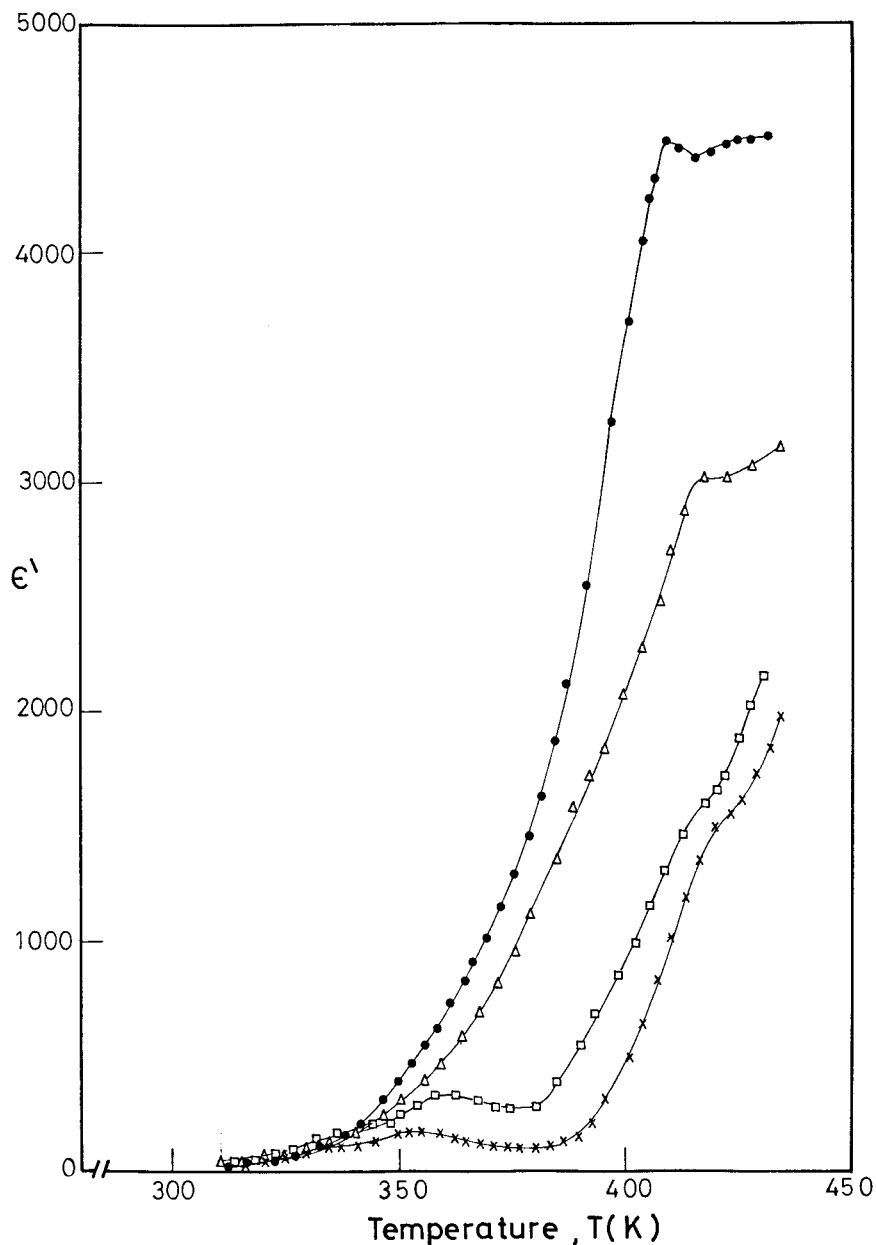


**Figure 6** The temperature dependence of  $\epsilon'$  for pure PVA at different  $\gamma$ -doses: ( $\times$ ) unirradiated, ( $\square$ )  $1 \times 10^4$  Gy, ( $\Delta$ )  $1 \times 10^5$  Gy, and ( $\bullet$ )  $2 \times 10^5$  Gy.

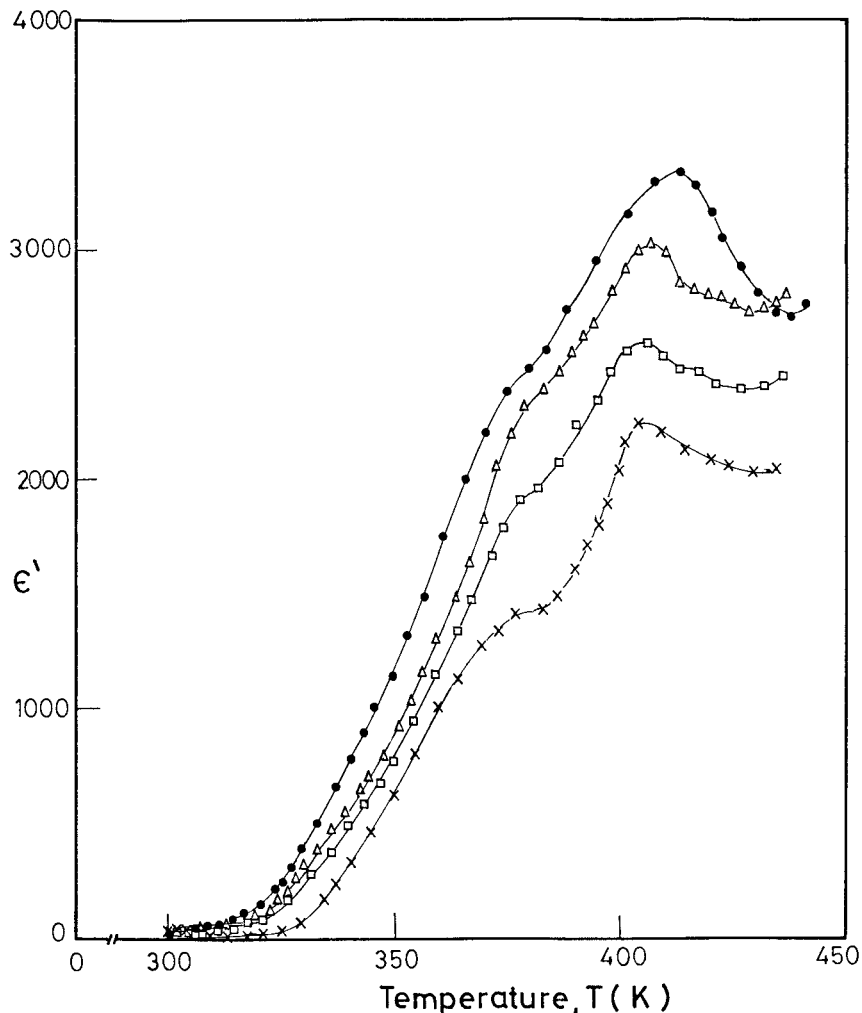
These molecular aggregates may be formed due to the inhomogeneous distribution of the dopant as well as the nonbonding part of the dopant.<sup>24,25</sup>

Figure 5 represents the variation of activation energy with  $\gamma$ -dose for all samples at low temperature regions I. Such a linear behavior obtained in Figure 5 and the insets of Figures 1–3 suggests further study of the possibility of using such a metal–polymer system as a  $\gamma$ -dosimeter through

the measured values of conductivity and activation energy.

#### Dielectric Constant

The dielectric properties of pure and  $\text{NiCl}_2$ -doped PVA samples, before and after irradiation, as function of temperature were studied. Figure 6 shows the variation of dielectric constant  $\epsilon'$  with



**Figure 7** The temperature dependence of  $\epsilon'$  for doped PVA with 5 wt %  $\text{NiCl}_2$  at different  $\gamma$ -doses: (x) unirradiated, ( $\square$ )  $1 \times 10^4$  Gy, ( $\Delta$ )  $1 \times 10^5$  Gy, and ( $\bullet$ )  $2 \times 10^5$  Gy.

temperature for pure PVA films at different  $\gamma$ -doses. The  $\epsilon'(T)$  curves for the unirradiated sample and that exposed to  $1 \times 10^4$  Gy  $\gamma$ -dose exhibit nearly similar dielectric behavior. A broad glass transition temperature  $T_g$  peak is appeared at about 355 and 360 K for the unirradiated and that irradiated at  $1 \times 10^4$  Gy, respectively. But the  $\alpha$ -relaxation temperature  $T_\alpha$  peak takes the shape of a shoulder around 420 K for both previously mentioned cases. For the irradiated samples at  $\gamma$ -doses  $1 \times 10^5$  and  $2 \times 10^5$  Gy, the glass transition peak disappeared while the  $\alpha$ -relaxation peak becomes more clear. The disappearance of the glass transition peak with irradiation may be attributed to structural changes in the polymer matrix, probably molecular and crystallographic rearrangement. In fact, gamma irradiation can pro-

duce different valency states of the transition metal ions in the matrix of the chelated compounds. At the same time, irradiation can affect the electronic state of the ligand molecules in the polymer matrix.<sup>14,26</sup> Starting from room temperature up to 350 K, the  $\epsilon'(T)$  curves themselves sometimes overlap and intersect. Above 350 K, the increase of  $\gamma$ -dose increases the magnitude of dielectric constant at different temperatures. The dielectric constant is strongly dependent on temperature at  $2 \times 10^5$  Gy  $\gamma$ -dose. Creation of carbonyl groups, which are highly polar, cause a remarkable increase in dielectric constant.<sup>27,28</sup>

The  $\epsilon'(T)$  curves for the samples containing 5 and 10 wt %  $\text{NiCl}_2$  show the same behavior. Accordingly, Figure 7 is given here as a representative of both. All curves exhibit a shoulder at the range



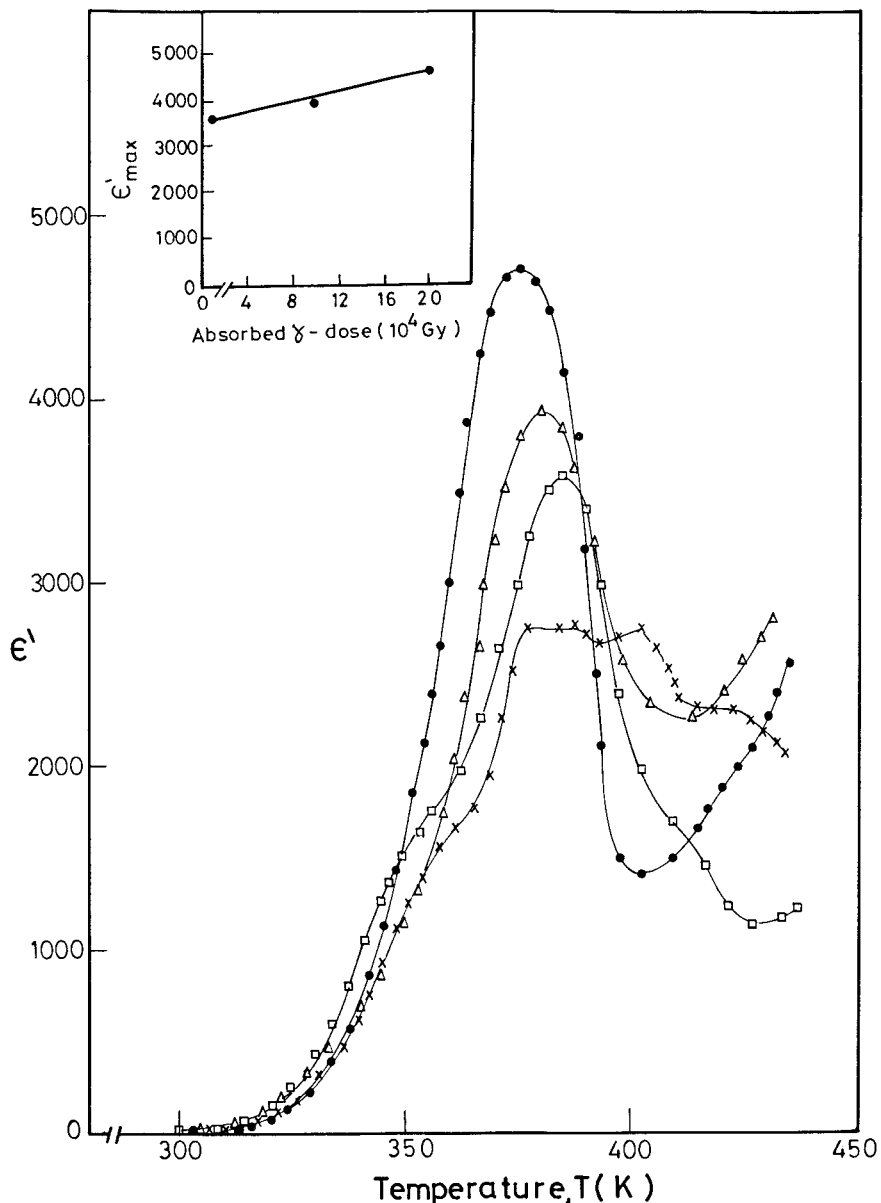


**Figure 8** The temperature dependence of  $\epsilon'$  for doped PVA with 20 wt %  $\text{NiCl}_2$  at different  $\gamma$ -doses: ( $\times$ ) unirradiated, ( $\square$ )  $1 \times 10^4$  Gy, ( $\Delta$ )  $1 \times 10^5$  Gy, and ( $\bullet$ )  $2 \times 10^5$  Gy.

of glass transition and a pronounced  $\alpha$ -relaxation peak, of which the prior shoulder decreases with increasing  $\gamma$ -dose. The position of the  $\alpha$ -relaxation peak for irradiated samples is shifted towards higher temperature values than the unirradiated one. The change in position of  $T_\alpha$  may be mainly to the effect of  $\gamma$ -irradiation on the orientation of the crystals, crystallinity, and microstructure of the sample. It is clear that the value of  $\epsilon'$  increases with increasing  $\gamma$ -dose over the whole temperature range. Besides crosslinking and degradation, evo-

lution of hydrogen may take place due to the irradiation of polymer material. The induced radiation effect on pure and doped polymer may decrease the disorder of the dipolar groups so the permittivity and the dielectric properties increase. However, the increase of the dielectric constant with temperature indicates that the dependence is governed mainly by the change in the intra- and intermolecular interactions.<sup>29</sup> These interactions may involve the alignment or rotation of the dipoles present in the polymer with temperature.

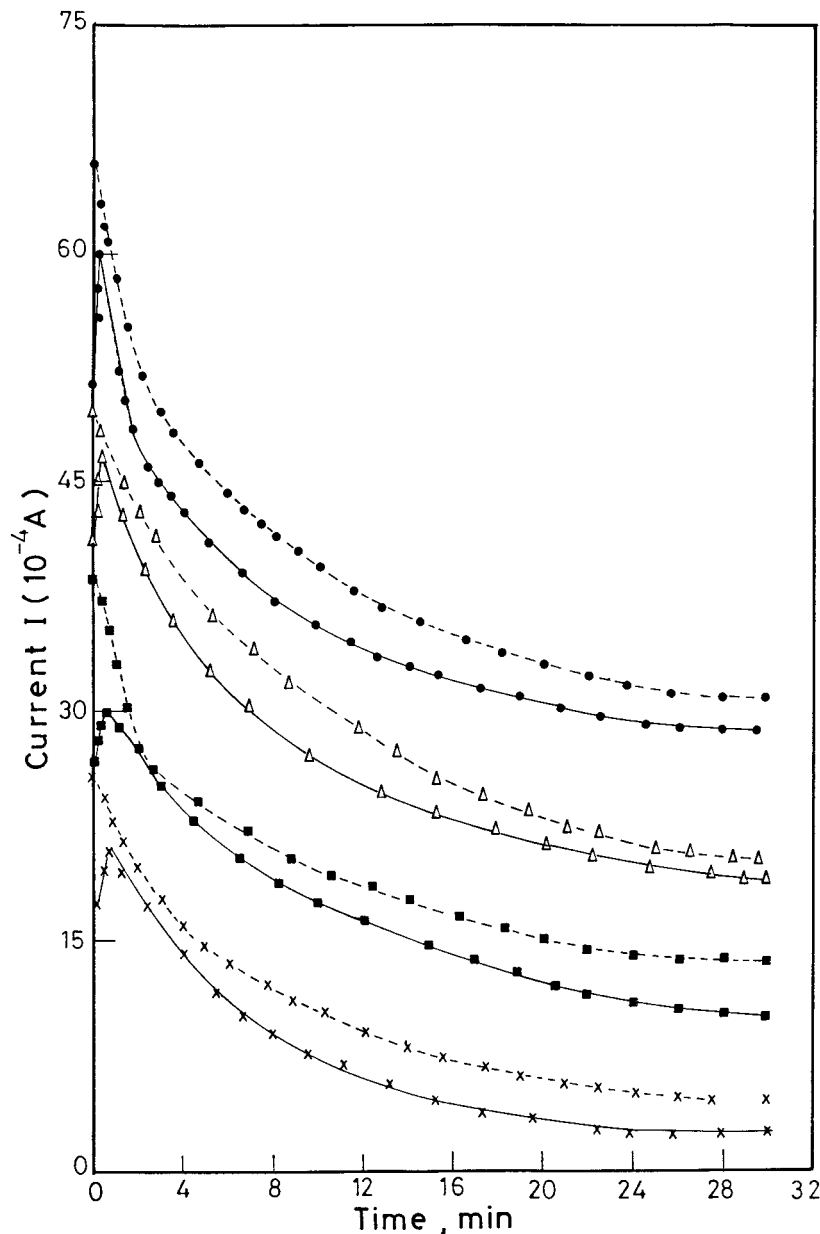


**Figure 9** Current relaxation curves for 5 wt %  $\text{NiCl}_2$ -doped PVA samples 0.25 mm thick at different  $\gamma$ -doses: ( $\times$ ) unirradiated, ( $\blacksquare$ )  $1 \times 10^4$  Gy, ( $\triangle$ )  $1 \times 10^5$  Gy, and ( $\bullet$ )  $2 \times 10^5$  Gy at 50 V and  $150^\circ\text{C}$ . Dotted lines refer to the first application of voltage, and the solid line refers to the reversed polarity.

The subsequent addition of transition metal halides to PVA matrix entails a considerable increase of  $\epsilon'$  at frequency of 1 kHz within the temperatures range used. This may be related to the effect of local environment on the inherent ability of the dipoles to orient.<sup>30</sup> Furthermore, it is possible to consider the effect of interfacial polarization, which exist only in a multiphase

system of inhomogeneous polymeric materials, in which the phase present possesses different permittivities and conductivities.<sup>31</sup> This agrees with the known fact that the large value of dielectric constant at the frequency used suggests that there is a contribution from all four known sources of polarization, namely, electronic, ionic, dipolar, and space charge polarization, of which

**Table II** Values of  $\mu$  ( $\text{cm}^2 \text{V}^{-1} \text{s}^{-1}$ ) and  $n$  ( $\text{cm}^{-3}$ ) for Pure, 5, 10, and 20 wt %  $\text{NiCl}_2$ -Doped PVA Samples (2.5 mm Thick) at Different  $\gamma$ -Doses

$\gamma$ -Doses	PVA		PVA + 5 wt % $\text{NiCl}_2$		PVA + 10 wt % $\text{NiCl}_2$		PVA + 20 wt % $\text{NiCl}_2$	
	$\mu$	$n$	$\mu$	$n$	$\mu$	$n$	$\mu$	$n$
Unirradiated	$7.10 \times 10^{-6}$	$2.81 \times 10^{18}$	$2.6 \times 10^{-7}$	$2.5 \times 10^{19}$	$2.10 \times 10^{-7}$	$2.60 \times 10^{19}$	$1.02 \times 10^{-7}$	$3.02 \times 10^{19}$
$1 \times 10^4$ Gy	$8.26 \times 10^{-6}$	$7.15 \times 10^{18}$	$2.98 \times 10^{-7}$	$3.14 \times 10^{19}$	$1.66 \times 10^{-7}$	$3.16 \times 10^{19}$	$1.02 \times 10^{-7}$	$3.22 \times 10^{19}$
$1 \times 10^5$ Gy	$9.12 \times 10^{-6}$	$9.20 \times 10^{18}$	$4.16 \times 10^{-7}$	$3.53 \times 10^{19}$	$2.76 \times 10^{-7}$	$3.24 \times 10^{19}$	$1.90 \times 10^{-7}$	$3.56 \times 10^{19}$
$2 \times 10^5$ Gy	$9.92 \times 10^{-6}$	$1.31 \times 10^{19}$	$5.2 \times 10^{-7}$	$3.61 \times 10^{19}$	$4.45 \times 10^{-7}$	$4.12 \times 10^{19}$	$2.21 \times 10^{-7}$	$3.68 \times 10^{19}$

the latter is known to contribute strongly at low frequencies.<sup>32</sup>

At relatively higher concentrations of dopants, namely 20 wt %  $\text{NiCl}_2$ , different  $\varepsilon'(T)$  curves are obtained, indicating the important role of metal halide additions, which cause structural variations in the polymeric network (see Fig. 8). A composite peak is observed for the unirradiated and that irradiated at  $1 \times 10^4$  Gy samples, while a broad Gaussian peak is observed for the irradiated samples at  $1 \times 10^5$  and  $2 \times 10^5$  Gy. The greater breadth of the relaxation can be attributed to the wider range of crystallite sizes. The peak position is found to be associated with a remarkable shift toward lower temperature. In addition, the maximum dielectric values  $\varepsilon'_{\text{max}}$  show a linear dependence of  $\gamma$ -exposure dose up to  $2 \times 10^5$  Gy (see the inset of Fig. 8).

### Current–Time Characteristics

The current–time curves for pure PVA and  $\text{NiCl}_2$ -doped samples before and after  $\gamma$ -irradiation at field strength  $200 \text{KV}_m^{-1}$  and temperature  $150^\circ\text{C}$  were measured. Similar plots were obtained, and, therefore, the current–time curves for 5 wt %  $\text{NiCl}_2$ -doped PVA samples are taken as a representative (Fig. 9). The observed relaxation phenomena can be attributed to two mechanisms. The first is the clean-up effect,<sup>33</sup> which is concerned with the effective decrease in the density of the mobile ions within the specimen due to their arrival at the electrode. The second mechanism is the effective drop of the electric field in the bulk of the specimen due to the space–charge effect of ions drifting to the electrode. The peaks observed in the reversed polarity curves (Fig. 9) can be explained as follows. A fraction of the ions that arrive at an electrode accumulate there as immobilized ions without discharging at the electrode.

These ions can become mobile again after the reversal of the polarity.

The order of magnitude of the drift mobility ( $\mu$ ) of charge carriers can be determined from the approximate relation, as follows:<sup>34,35</sup>

$$\tau \simeq t_{\text{max}} = d^2/\mu V \quad (3)$$

where  $d$  is the thickness of the sample,  $V$  is the applied voltage, and  $\tau \simeq t_{\text{max}}$  is the relaxation time corresponding to the peak current in  $I-t$  curve. Also, the charge carrier density  $n$  can be calculated from the following equation:

$$J = nq\mu E \quad (4)$$

where  $J$  is the current density at field strength  $E$ , and  $q$  is the carrier charge.

The obtained results are presented in Table II. The value of drift mobility is very low and decreases with the increase of subsequent addition of nickel chloride to PVA, indicating predominant ionic conduction.<sup>36</sup> Besides, it can be deduced that conduction enhancement is apparently due to the gradual increase of bulk-generated free carriers, density  $n$ . Moreover, mobilities smaller than  $1 \text{cm}^2 \text{V}^{-1} \text{s}^{-1}$ , which is the case in Table II, indicate that polaron hopping between localized sites is involved in the process of carrier transport. On the other hand, the increase of drift mobility with  $\gamma$ -dose indicates that the conduction is apparently due to thermally activated mobility. This seems to be consistent with electrical conductivity data.

### CONCLUSION

It is worthy to mention that the irradiation of polymers and the addition of dopant give rise to changes in electrical characteristics such as con-

ductivity and dielectric constant. Irradiation of polymers generally increases their electrical conductivity and decreases the activation energy. This can be explained on the basis that during irradiation, ions and free radical are formed and then trapped in the bulk of the material. In addition, electrons are excited to an essentially free state (conduction band) to produce electrical conduction.

The conduction current and the dielectric constant values are composition- and  $\gamma$ -radiation-dependent. The linearity obtained between the conductivity, activation energy at low temperature region *I*, and  $\epsilon'_{\max}$  for 20 wt % NiCl<sub>2</sub> with  $\gamma$ -doses reflects the importance of using such a metal-polymer system as the  $\gamma$ -ray dosimeter in the studied dose range. However, this prediction needs more work to be elucidated.

## REFERENCES

1. D.R. Garel, P. Gaudreau, and L. M. Zhong et al., *J. Surg. Res.*, **51**, 297 (1991).
2. K. Inoue, J. Fujisato, and K. Eurezak et al., *Pancrease*, **7**, 562 (1992).
3. N. P. Peppas and E. W. Merrill, *J. Biomed. Mater. Res.*, **11**, 423 (1977).
4. P. D. Garrett and D. T. Grubb, *J. Polym. Sci., Part B: Polym. Phys.*, **26**, 2509 (1988).
5. A. F. Basha, M. Amin, K. A. Darwish, and H. A. Abdel Samed, *Indian J. Polym. Mater.*, **5**, 115 (1988).
6. A. F. Basha, M. Amin, H. A. Abdel Samed, and K. A. Darwish, *Indian J. Polym. Mater.*, **5**, 161 (1988).
7. G. K. Narula, A. Tripathi, and P. K. C. Pillai, *J. Mater. Sci.*, **26**, 4130 (1991).
8. J. Kurkijarvi, *Phys. Rev. B*, **8**, 922 (1973).
9. J. Kurkijarvi, *Phys. Rev. B*, **22**, 2099 (1980).
10. A. K. Sharma, V. Adinarayara, and D. Santhi Sagar, *J. Mater. Lett.*, **12**, 247 (1991).
11. H. S. Nalwa, *J. Mater. Sci.*, **27**, 210 (1992).
12. F. H. Abd El-Kader, G. Attia, and S. S. Ibrahim, *J. Appl. Polym. Sci.*, **50**, 1281 (1993).
13. Y. Tanaka, Y. Mita, Y. Ohki, H. Yoshioka, M. Ikeda, and F. Yazaki, *J. Phys. D: Appl. Phys.*, **23**, 1491 (1990).
14. F. H. Abd El-Kader, S. S. Hamza, and G. Attia, *J. Mater. Sci.*, **28**, 6719 (1993).
15. F. H. Abd El-Kader, G. Attia, and S. S. Ibrahim, *J. Polym. Degrad. Stab.*, **43**, 253 (1994).
16. X. Lu, N. Brown, M. Shaker, and I. L. Kamel, *J. Polym. Sci., Part B: Polym. Phys.*, **33**, 153 (1995).
17. C. A. Hogarth and M. J. Bosha, *J. Phys. D: Appl. Phys.*, **16**, 869 (1983).
18. C. Muralidhar and P. K. C. Pillai, *J. Mater. Sci. Lett.*, **6**, 439 (1987).
19. C. Bowlt, *J. Phys. D: Appl. Phys.*, **16**, L 101 (1983).
20. T. W. Wilson, R. E. Fornes, R. D. Gilbert, and J. D. Memory, *J. Polym. Sci., Part B: Polym. Phys.*, **26**, 2029 (1988).
21. G. N. Bobu and J. C. W. Chien, *Macromolecules*, **17**, 2761 (1984).
22. B. Z. Tang, T. Masuda, and J. Higashimura, *J. Polym. Sci., Part B: Polym. Phys.*, **28**, 281 (1990).
23. P. Huo and P. Cebe, *J. Polym. Sci., Part B, Polym. Phys.*, **30**, 239 (1992).
24. A. K. Sharma, B. Rukmini, and D. Santhi Sagar, *J. Mater. Lett.*, **12**, 59 (1991).
25. N. Venugeopl Reddy and V. V. R. Narasimha Rao, *J. Mater. Sci. Lett.*, **11**, 1036 (1992).
26. L. D. Bogmolova, A. G. Fedorov, V. A. Jach Kin, and V. N. Lazukin, *J. Mater. Sci. Lett.*, **37**, 381 (1980).
27. S. Cygan and J. R. Laghari, *IEEE Trans. Nucl. Sci.*, **36**, 1386 (1989).
28. S. A. Gaafar, F. H. Abd El-Kader, and M. S. Risk, *Physica Scripta*, **49**, 366 (1994).
29. A. K. Sharma and Ch. Ramu, *Mater. Sci. Lett.*, **11**, 128 (1991).
30. A. Tager, *Physical Chemistry of Polymers*, Mir Publishers, Moscow, 1972.
31. P. J. Philips, *Electrical Properties of Solid Insulating Materials*, Vol. II, ASTM Book Series of Engineering Dielectrics, ASTM, Philadelphia, 1980.
32. G. Prasad and K. V. Rao, *Phys. Status Solidi A*, **97**, 455 (1986).
33. M. Koski and S. M. Ceda, *Jpn. J. Phys. Soc.*, **29**, 1012 (1970).
34. S. Isoda, H. Mjiaji, and K. Asai, *Jpn. J. Appl. Phys.*, **12**, 1799 (1973).
35. K. Jain, A. C. Rastogi, and K. L. Chopra, *Phys. Status Solidi A*, **20**, 167 (1973).
36. V. K. Jain, C. L. Gupta, and N. K. Jain, *Ind. J. Pure Appl. Phys.*, **16**, 625 (1978).